Available online at www.sciencedirect.com

ScienceDirect

Advances in Space Research 74 (2024) 4793–4808

ADVANCES IN SPACE RESEARCH (a COSPAR publication)

www.elsevier.com/locate/asr

Changes in general circulation of the middle and upper atmosphere associated with main and transitional QBO phases

A.V. Koval [a,b,*], K.A. Didenko [c,a], T.S. Ermakova [b,a], N.M. Gavrilov [a], A.V. Sokolov [a]

[a] Atmospheric Physics Department, Saint Petersburg University, Saint Petersburg, Universitetskaya nab 7-9, Russia
[b] Meteorological Forecast Department, Russian State Hydrometeorological University, Saint Petersburg, Voronezhskaya Street 79, Russia
[c] Pushkov Institute of Terrestrial Magnetism, Ionosphere and Radio Wave Propagation RAS (IZMIRAN), Troitsk, Kaluzhskoe Highway 4, Russia

Received 13 June 2024; received in revised form 11 July 2024; accepted 13 July 2024
Available online 18 July 2024

Abstract

Three-dimensional numerical nonlinear model of general circulation of the middle and upper atmosphere (MUAM) is used to simulate changes in the atmospheric dynamical and thermal regimes related to changes in phases of equatorial stratospheric quasi-biennial oscillation (QBO). In addition to conventional (easterly and westerly) QBO phases, two transitional: westerly-shear (wsQBO, from easterly to westerly) and easterly-shear (esQBO, from westerly to easterly) QBO phases are added into consideration in order to research in details QBO-induced changes in global circulation and interactions of planetary waves (PWs) with the mean flow. To interpret the obtained results, the residual meridional circulation, Eliassen-Palm fluxes and meridional temperature gradients are calculated based on MUAM ensemble simulations for the four QBO phases. The simulation results showed different temperature and zonal wind structures in the extratropical winter stratosphere at different QBO phases. The esQBO transition phase is characterized by the strongest temperature and zonal wind changes. This is obtained both from the simulation and from the reanalysis data, and can be explained by PW influence directly through changes in Eliassen-Palm flux and indirectly through modifications in the meridional circulation. Abrupt changes in the subpolar stratosphere during esQBO are gradually compensated for the next 3 phases. Changes in the zonal wind in the thermosphere due to the QBO phases changes can reach 10 %. An increase in wave activity in the Northern Hemisphere is accompanied by a weakening of the zonal wind during the esQBO and eQBO phases above approximately 150 km.

Keywords: Quasi-biennial oscillation; Numerical modeling; Residual circulation; General atmospheric circulation

1. Introduction

The quasi-biennial oscillation (QBO) of the equatorial zonal wind is one of the important processes influencing the atmospheric dynamics (e.g., Baldwin et al., 2001). The QBO arises at low latitudes: the direction of the zonal wind in the equatorial stratosphere changes to the opposite within time interval between 22 and 34 months. Back in the 80s, Holton and Tan began to analyze the response of the extratropical circulation to the QBO (Holton and Tan, 1980). They proposed a mechanism of modulation of the Northern Hemisphere wintertime stratospheric polar vortex by QBO through the changing width of the planetary wave (PW) waveguides and concluded that during northern

* Corresponding author at: Saint Petersburg University, Saint Petersburg, Universitetskaya nab 7-9, Russia.
E-mail addresses: a.v.koval@spbu.ru (A.V. Koval), didenko.xeniya@yandex.ru (K.A. Didenko), taalika@mail.ru (T.S. Ermakova), n.gavrilov@spbu.ru (N.M. Gavrilov), anigahuchi@yandex.ru (A.V. Sokolov).

https://doi.org/10.1016/j.asr.2024.07.037

winter the eastward zonal mean jet is weaker and more disturbed during the easterly QBO phase (eQBO) than that during the westerly QBO phase (wQBO).

This mechanism has been repeatedly studied and refined (e.g., Anstey and Shepherd, 2014 and references therein). By now, it is clear that the Holton-Tan mechanism is only one of many others that explains QBO influence on extratropical atmospheric dynamics. For example, Garfinel et al. (2012) used numerical simulations and showed that the changes in meridional circulation associated with QBO are important for the formation of the polar vortex. However, this conclusion does not lessen the importance of studying the of PW – mean flow interaction, since meridional circulation, in turn, is generated by atmospheric waves in accordance with the "Downward control principle" (Haynes et al., 1991).

Gavrilov et al. (2015) performed numerical modeling to study planetary waves (PWs) and orographic gravity waves (OGWs) interactions in the middle and upper atmosphere during easterly and westerly QBO phases for January and February. They showed that changes in atmospheric circulation caused by QBO are associated with significant changes in PW amplitudes in the extratropical stratosphere and mesosphere. A broad review of a history and recent achievements in studying the influence of the QBO on the low-latitude upper troposphere and lower stratosphere is presented by Hitchman et al. (2021). Influence of equatorial stratospheric QBO in the form of a quasi-biennial cyclicity was found in all hydrodynamic fields (temperature, pressure, wind components, etc.) at middle and high latitudes and altitudes up to the thermosphere (e.g., Wang et al., 2018; Koval et al., 2022a). In particular, Wang et al. (2018) showed that the impact of stratospheric QBO at thermospheric altitudes is weaker compared to the quasi-biennial oscillation of solar activity, especially during the solar maximum. Nevertheless, as calculated by Koval et al. (2022a), this contribution is statistically significant and can induce noticeable changes in the circulation at the solar minimum. The propagation of the stratospheric QBO signal into the ionosphere and the associated variations in the critical frequency foF2 have been considered also by Echer (2007).

A large number of publications in recent years confirms the continuing interest in studying various aspects of atmospheric dynamics associated with QBO. A detailed review of the state of the art in QBO modeling was recently presented by Richter et al. (2020). Among the recent studies dedicated to the research of QBO effects based on meteorological reanalysis, the following should be highlighted: Alsepan et al. (2016) performed analysis of the lower stratosphere QBO according to ECMWF data and showed that QBO has a significant effect on the total column ozone, with its increase during wQBO and decrease during eWBO; Ribera et al. (2004) distinguished secondary meridional circulation caused by QBO using singular vector decomposition applied to NCEP–NCAR reanalysis. This secondary circulation is characterized by temperature anomalies associated with adiabatic vertical motions over zones of zonal wind shear. The study of QBO and its reproduction in climate models within the framework of the SPARC QBO-initiative is described by Bushell et al. (2020). The long-term changes in the northern midwinter temperature, zonal wind and residual circulation, associated with QBO, were studied by Gabriel (2019). In particular, their study is dedicated to finding the relationship between the QBO and the growth of greenhouse gases observed in recent decades, as far as both of these processes affect extratropical circulation. Their results based on numerical simulations with the Earth-System Models involved into the "Coupled Model Intercomparison Project Phase 5" (CMIP5, Giorgetta et al., 2013) showed a gradual shift of the extratropical wQBO signature towards the eQBO signature projected over the 21st century if greenhouse gases continue to increase.

Recently, based on the numerical simulations with the GCM MUAM, Koval et al. (2022a) demonstrated how changes in the PW structures promote spread of QBO effects to polar latitudes and to the thermosphere, through changes in the Eliassen-Palm (EP) flux and its divergence (e.g., Trenberth, 1986) and through the formation of wave-induced eddy meridional circulation. They showed, in particular, that the main contribution to the cooling of the polar winter stratosphere during the wQBO was associated with the weakening of PW activity. In addition, during the westerly QBO phase, weakening of meridional circulation, accompanying by a temperature increase occurs in the thermosphere.

A number of papers (Wallace et al., 1993; Fraedrich et al., 1993; Solomon, 2014; Hitchman et al., 2021) consider more QBO stages in addition to conventional westerly and easterly QBO phases. Koval et al. (2022a) determined the QBO phases using decomposition of observed equatorial zonal wind variations with empirical orthogonal functions (EOF). This approach allowed to determine that different QBO phases existed in January-February of different years taking into account vertical evolution of the zonal flow at altitude range between 1 and 70 hPa. Four QBO phases were defined as follows: easterly (eQBO), westerly (wQBO) and transitional (so-called easterly-shear and westerly-shear, esWBO and wsQBO, respectively). Despite extensive experience in determining transitional QBO phases (see Hitchman et al., 2021 and references therein), no detailed analysis of changes in the general atmospheric circulation and PW interaction with mean flow during QBO transitional phases has been carried out to date.

The current study is dedicated to studying the interaction of PWs with the mean flow, the ability of PW to transmit the signal from the QBO into the layers of the thermosphere and into high-latitude regions. Koval et al. (2022a) made similar analysis for the classical eQBO and wQBO phases. In this paper, this analysis was extended by taking into account all four QBO phases mentioned above. To analyze of the interaction of PWs with the mean flow, Eliassen-Palm flux, its divergence, as well as the com-

ponents of the residual mean meridional circulation are considered. Also, we analyzed in which phases the direct effect of the PW plays the main role in the change in circulation (through the Holton-Tan mechanism), and in which ones – the indirect effect (through the change in the meridional circulation) dominates. The use of numerical simulation for different QBO phases observed in January-February allowed us to study pure QBO effects rectified from possible contributions of seasonal variations, which could affect the results of simulations.

2. Methodology

To simulate global atmospheric circulation and estimate changes in dynamical and thermal regimes, the middle and upper atmosphere model (MUAM) was used. This is a 3-dimensional nonlinear mechanistic numerical model based on the circulation model COMMA created at the University of Cologne, Germany (Ebel et al., 1995) and its further development of COMMA-LIM (Fröhlich et al., 2003), with numerous modifications described in later studies (Pogoreltsev et al., 2007; Jacobi et al., 2017; Ermakova et al., 2019; Koval et al., 2022a). The horizontal grid of the model is 5.625°x 5° in longitude and latitude, respectively. The MUAM uses a log-isobaric vertical coordinate $z = -H*\ln(p/p_o)$, where p_o is the surface pressure and H is pressure scale height. The current MUAM version has 56 vertical levels covering altitude range from the surface up to about 300 km. The detailed scheme of numerical experiments with actual MUAM version is described by Koval et al. (2021; 2022a). The ability of MUAM to correctly reproduce atmospheric circulation, tides, and planetary waves has been repeatedly discussed in previous publications by comparison with reanalysis data and empirical models (e.g., Suvorova and Pogoreltsev, 2011; Koval et al., 2019; 2021; 2022a).

To prepare background and initial conditions for the present simulations, we determine QBO phase using the decomposition of zonal wind variations from MERRA-2 reanalysis data (Gelaro et al., 2017) with EOFs. The QBO signal in the field of the monthly-mean equatorial zonal wind after subtracting seasonal cycle is decomposed into two main orthogonal functions in the altitude range of 1–70 hPa. Further, these two principal components are considered and their scattering diagram is subdivided into 4 patterns corresponding to different QBO phases (Koval et al., 2022a). This approach allows taking into account vertical evolution of QBO phases and minimize uncertainties in determination of the QBO phases. Similar methodology of defining QBO phases was used also by Hitchman et al. (2021), who studied the influence of the QBO to the heights of the lower stratosphere. In addition to eQBO and wQBO phases (when zonal wind vertical shear du/dz is close to 0, in this study we consider the "easterly-shear" (esQBO) phase, which is a transition between the westerly and easterly QBO, when an easterly wind shear is negative ($du/dz < 0$) at the level of 20 hPa (see Fig. 2 below). Accordingly, the "westerly-shear" (wsQBO) phase with $du/dz > 0$ is a transition between easterly and westerly QBO. We have chosen the 20 hPa level designate, because this level corresponds to the observed maximum of root-mean-square deviation of the zonal wind velocity. Maximum amplitude of the zonal wind QBO at 20 hPa calculated based on reanalysis data one can see in Fig. 4a of the paper by Alsepan et al. (2016). In the study by Koval et al. (2022b), the years were selected, when each of mentioned above four QBO phases were observed in January based of zonal wind fields from MERRA-2. These years are presented in Table 1. Koval et al. (2022b) performed test numerical simulations in order to estimate changes in the meridional circulation caused by the QBO. In the current study, the ensembles of model runs are extended to improve statistical significance and provide a more detailed analysis of QBO-modulated PW-mean flow interactions. To provide feedback on previous studies, we checked the correspondence of the QBO phases obtained by us with the QBO index developed in Singapore (Singapore QBO index), which is widely used nowadays and represents the sum of the monthly mean zonal wind at vertical levels between 10 and 70 hPa (e.g. Wang et al, 2017). In this conventional QBO classification, the easterly QBO phase corresponds to our esQBO and eQBO phases, while the conventional westerly QBO phase corresponds to our wsQBO and wQBO phases.

To date, several different methods have been developed for determining QBO phases, which differ in the height of determining the wind direction and/or number of levels used for determining QBO (e.g., Hamilton, 1998; Baldwin et al., 2001; Huesmann and Hitchman, 2001; White et al., 2015; Gavrilov et al., 2015 and references therein). In general, the westerly and easterly QBO zones determined at pressure levels 10–20 hPa may have substantial phase shifts compared to the same zones obtained, for instance, at 50–70 hPa. One should keep in mind such vertical phase shifts, when comparing QBO phases determined at different pressure levels.

For years listed in Table 1, distributions of average zonal-mean zonal wind and temperature for all four QBO phases were calculated and implemented into MUAM using nudging in the equatorial stratosphere (see Pogoreltsev et al., 2014; Koval et al., 2022a for details). Such approach of analyzing different QBO phases in the same month allows us to eliminate influence of seasonal variations and rectify impacts of QBO phases only. Pogoreltsev et al. (2014) proposed to use additional terms in MUAM equations for zonal wind velocity and temperature, which are proportional to differences between calculated and observed zonal mean winds at latitudes from 17.5°S to 17.5°N and altitudes from 0 to 50 km. Such approach implying relaxation of the modeled low-latitude zonal wind and temperature fields to the observations is needed, as far as MUAM cannot reproduce QBO phases internally due the relatively low vertical resolution. Vertical grid of the MUAM is around 2.8 km in the lower and mid-

Table 1
Years of observations of four QBO phases in January, obtained using EOF decomposition of the MERRA-2 meteorological reanalysis data.

wQBO	esQBO	eQBO	wsQBO
1983, 1985, 1993, 1995, 1999, 2002, 2004, 2013	1981, 1986, 1991, 2007, 2009, 2011, 2014, 2016	1989, 1996, 1998, 2000, 2003, 2005, 2010, 2012	1980, 1990, 1992, 1997, 2001, 2006, 2008, 2015

dle atmosphere along log-pressure coordinate, however, as Geller et al. (2019) showed, to correctly reproduce the QBO in the model and take into account gravity waves momentum deposition, the vertical resolution must be at least 500 m in the lower stratosphere. The disadvantages associated with coarse grid, however, is compensated by saving computing time, since MUAM is a simple mechanistical model. Another important advantage of MUAM is its ability to reproduce the resonant properties of the atmosphere (atmospheric normal modes, NMs), which is necessary when studying large-scale atmospheric interactions, as in the current work (e.g., Pogoreltsev, 2007).

To study the thermodynamic state of the atmosphere associated with vertical and meridional motions, the calculation of the residual meridional circulation (RMC) is performed. RMC is introduced within transformed Eulerian mean framework (TEM, Andrews and McIntyre, 1976). It is a superposition of advective transport and wave-induced eddy motions. Analyzing RMC provides diagnostics of wave impacts on the mean flow and gives the ability to assess meridional transport of mass and long-lived species in the atmosphere. In contrast to the zonal-mean Eulerian circulation, the residual vertical velocity is proportional to the net rate of diabatic heating (e.g., Shepherd, 2007). More detailed description of method for calculating RMC based on MUAM data, including respective formulas, is presented in (Koval et al., 2021).

For a deeper analysis of atmospheric dynamic processes, it is necessary to take into account the exchange of energy and momentum between atmospheric mean flows and waves, since QBO modulates PWs. For this purpose, meridional and vertical components of the Eliassen-Palm flux (EP flux), $F_m = (F_m^{(\varphi)}, F_m^{(z)})$, and its divergence, ∇F_m, are calculated using formulas (e.g., Andrews et al., 1987):

$$F_m^{(\varphi)} = cos\varphi \left(\bar{u}_z \frac{\overline{v'\theta'}}{\bar{\theta}_z} - \overline{u'v'} \right) \quad (1)$$

$$F_m^{(z)} = cos\varphi \left(\left(f - \frac{(\bar{u}\, cos\varphi)_\varphi}{a cos\varphi} \right) \frac{\overline{v'\theta'}}{\bar{\theta}_z} - \overline{w'u'} \right) \quad (2)$$

$$\nabla F_m = \frac{1}{a cos\varphi} \frac{\partial}{\partial \varphi} \left(F_m^{(\varphi)} cos\varphi \right) + \frac{\partial F_m^{(z)}}{\partial z} \quad (3)$$

where, overbars and primes denote zonaly averaged values and deviations from the zonaly averaged values (disturbances), respectively; indices show partial derivatives; u, v and w are zonal, meridional and vertical wind components; $\theta = Texp(\frac{g}{Cp} \int_0^h \frac{\mu}{T} dh)$ is potential temperature; C_p is the heat capacity at constant pressure; h is the geopotential height; f is the Coriolis parameter; φ is latitude.

The EP flux divergence is interpreted as net drag of the zonal-mean flow by PWs and vertical EP flux component is associated with meridional heat flux.

To achieve statistical significance of the simulations, four series (ensembles), each containing 12 calculations ("runs") with the MUAM model were obtained for conditions typical for the observed four QBO phases using nudging. The scheme of numerical experiments is as follows. Each MUAM simulation within the ensemble starts from an initial windless atmosphere with the climatological globally averaged vertical temperature profile. During the first 30 model days, gravity-wave parameterizations in the model are not included and geopotential heights at the lower boundary do not change. Then, the longitudinal geopotential variations (stationary planetary waves) are specified. Within the first 120–131 days, the MUAM uses daily averaged heating rates. Pogoreltsev (2007) showed that the described procedure allows the model to reach steady-state regime at the end of this time interval. After a day between 120 and 131, daily variations of heating and sources of atmospheric NMs are included. By changing the date of inclusion of NM sources between 120 and 131 model days with a step of 1 day, we shift the phase of stratospheric vacillations (e.g., Holton and Mass, 1976; Pogoreltsev, 2007). Starting from the 300th model day, seasonal changes in the zenith angle of the Sun are launched, and days 330–360 correspond to January. It should be noted that the monthly-mean PW amplitudes, the intensity of the mean flow, and the temperature in the stratosphere in winter from one run to another can change significantly. Changes between model runs are interpreted as interannual variability (Pogoreltsev, 2007). Features of creating the ensembles based on changes in stratospheric vacillation cycles as well as statistical data processing are described in detail by Koval (2019). Comparing simulated hydrodynamic fields with the MERRA-2 for the sets of years listed in Table 1 shows good agreement (see below). Our simulations are consistent also with the results of Rao et al. (2019) who investigated the structure of stratospheric circulation based on 10 reanalyzes of meteorological information and numerical simulations.

Fig. 1 shows the averaged over January differences (increments between zonal wind and temperature fields obtained for successive QBO phases according to the MERRA-2 reanalysis data. For each QBO phase, the differences are averaged over set of years listed in Table 1. The downward shifting QBO phase (in the form of

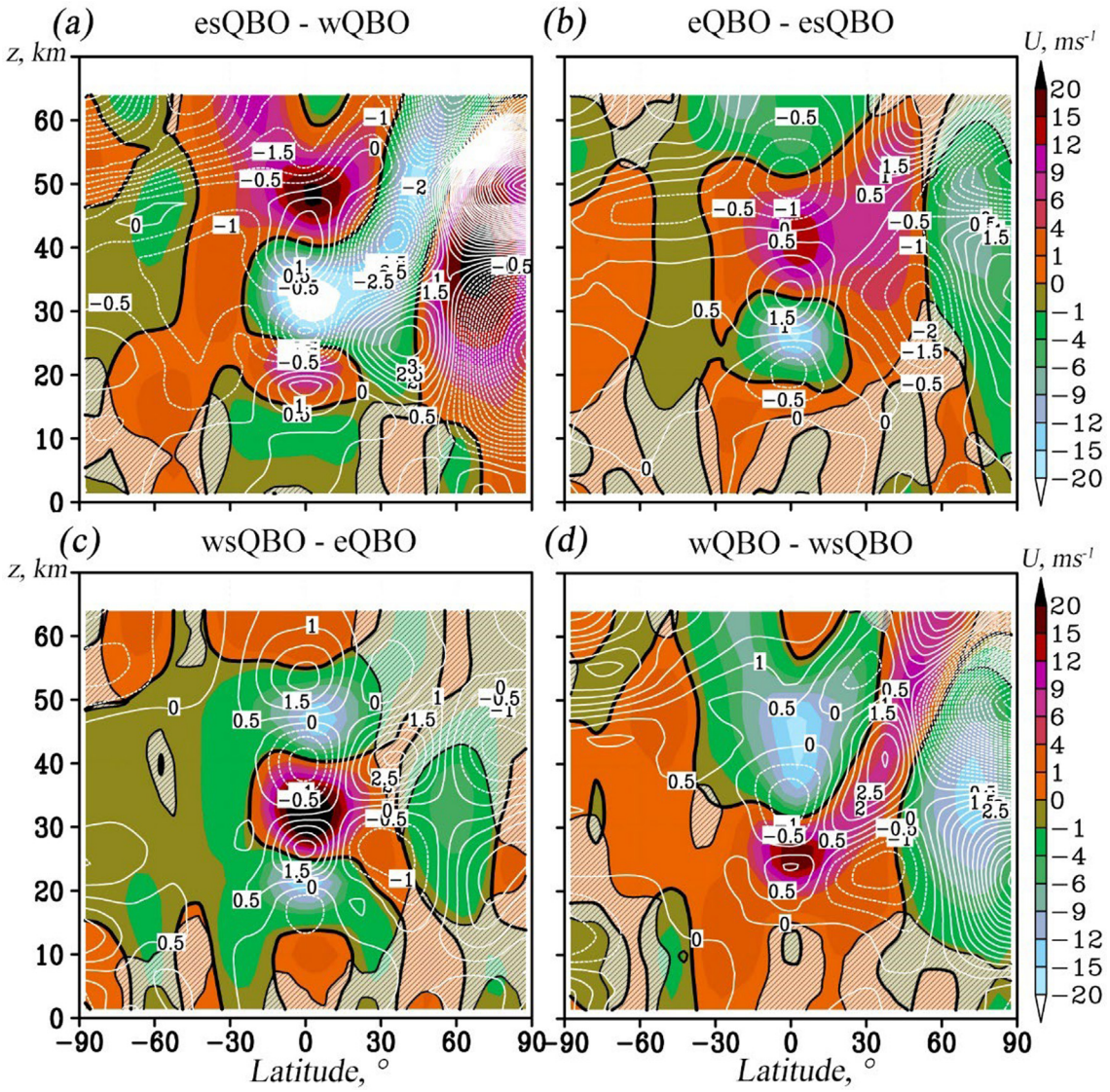

Fig. 1. Latitude-height distributions of the differences between successive QBO phases of zonal-mean zonal wind (shaded, m/s) and temperature (contours, K) according to MERRA-2 for January. Hatched areas show insignificant wind increments at 95%.

increments of the zonal wind and temperature) is well distinguishable in the equatorial region. For example, in Fig. 1a, the zonal wind increments are negative in the altitude range of 25–40 km, and are positive in areas above and below this range. In Fig. 1b-d, these areas gradually descend. The background temperature also changes accordingly. As noted in earlier studies (e.g., Choi et al., 2002; Hitchman et al., 2021 and references therein), at the equatorial latitudes, cooling corresponds to easterly wind shear, and heating corresponds to westerly wind shear (see, for example, Fig. 1a, altitude intervals of 20–35 km and 35–50 km, respectively). Such temperature changes are primarily due to vertical motions: weakening (strengthening) of equatorial upwelling causes adiabatic heating (cooling). At the same time, compensatory processes occur outside the equatorial region which is a consequence of the impact of the secondary meridional circulation, considered, for example by Choi et al. (2002); Ribera et al. (2004): in Fig. 1a at 30° N, regions with opposite temperature changes associated with opposite changes in vertical motions are clearly distinguishable. Similar processes can be traced in all panels of Fig. 1. The distributions of the zonal wind and temperature, which differences are presented in Fig. 1, are implemented into the MUAM to nudge the circulation to the corresponding QBO phase.

3. Results of numerical simulations

As it was described above, model simulations were performed for January for all of four QBO phases, at altitudes from the surface up to 200 km. The month of January was chosen due to the fact that during the winter season the PW wave activity increases, and in this study, we consider the change in the general circulation primarily from the point

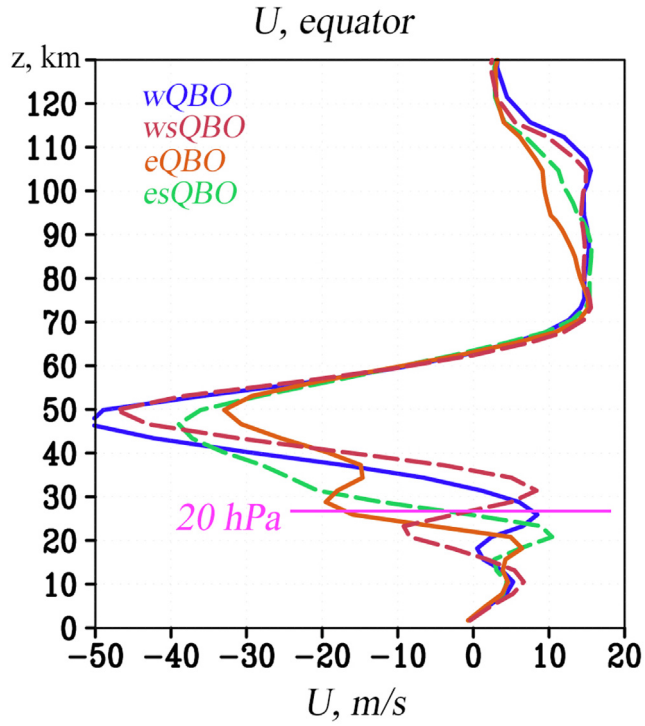

Fig. 2. Vertical profile of the zonal-mean equatorial zonal wind for all QBO phases. Dashed lines show shear phases.

of the PW – mean flow interaction. In addition, as discussed in earlier papers such as Baldwin and O'Sullivan (1995), the QBO effect is stronger in December and January, weakening by February. For each QBO phase, an ensemble of model simulations consisting of 12 members was obtained. These data were averaged and statistically processed.

Fig. 2 shows vertical profiles of the zonal mean zonal wind averaged over the equatorial region (±2.5°) for the four QBO phases considered. As was shown by Koval et al. (2022a), the QBO phase is determined by the direction of the main component of the EOF expansion of the equatorial zonal wind field at the pressure level of 20 hPa (indicated in Fig. 2 by the pink line). It is clearly seen that at this level the zonal wind is directed eastward and westward for the wQBO and eQBO, respectively. For the transitional phases the wind shear towards the next phase is observed, while the value of zonal wind is close to zero. I.e., for the esQBO and wsQBO, easterly wind shear ($du/dz > 0$) and westerly wind shear ($du/dz < 0$) are seen in the green and red lines in Fig. 2, respectively. At altitudes up to 60 km, significant differences between zonal wind profiles for different QBO phases are seen in Fig. 2, which results in positive and negative wind differences discussed further. In Fig. 2 one can also see larger variability of the equatorial zonal wind at altitudes of 80 – 120 km, which is primarily associated with significant variability in the meridional circulation between different QBO phases.

The top panels of Fig. 3 show the latitude-altitude distributions of the zonal mean zonal wind and temperature, simulated with the MUAM model for January for the wQBO. In general, the distributions correspond both to the MERRA-2 reanalysis of meteorological information for years with the wQBO (see Table 1), and to semi-empirical atmospheric models such as HWM-14 (Drob et al., 2015) and NRLMSIS 2.0 (Emmert et al., 2020). Contours in Fig. 3a show the divergence of EP flux. Positive EP flux divergence should be accompanied by an eastward acceleration of the zonal wind caused by PW momentum transfer to the mean flow, while negative divergence (i.e., convergence) corresponds to a zonal wind deceleration. Vectors in Fig. 3b show RMC components. The RMC is currently widely used to estimate the meridional transport of long-living and passive atmospheric species. In the stratosphere, the RMC represents branches of Brewer-Dobson circulation (Butchart, 2014), with ascending flows in the low-latitude region and descending flows at high latitudes, and the northern (winter) circulation cell is much stronger than the southern (summer) one. In the mesosphere and thermosphere, the transfer of air masses from the summer to winter hemisphere dominates.

To analyze changes in the atmospheric circulation, we also consider the vertical component of the EP flux, Fz, and meridional thermal gradient, which are shown in Fig. 3c, d for the wQBO phase. Atmospheric PW theory (e.g., Andrews et al., 1987) shows that the upward EP flux coincides with the poleward wave heat flux, and its enhancement can cause warming of the atmosphere in extratropical regions. The structure of Fz in Fig. 3c is typical for boreal winter: the EP flux is maximal in the winter middle atmosphere (below 100 km). In this region, both the amplitudes of quasi-stationary PWs and of long-period atmospheric NMs are maximum (e.g., Koval et al. 2018; 2019). The barrier region of negative Fz at a height of 100–120 km does not allow direct PW propagation into the upper atmospheric layers. Latitude-altitude distributions of hydrodynamical parameters shown in Fig. 3 for all 4 QBO phases are presented in Supplement, in Figs. S1-S4.

In the MUAM equations of motion, in accordance with the classical theory of "thermal wind" (e.g., Gill, 1986), the vertical gradient the zonal (meridional) wind is proportional to the meridional (zonal) temperature gradient. In the Northern Hemisphere, a positive increment in the meridional temperature gradient corresponds to a westward (negative) zonal wind shear. Most of the temperature gradient distribution in Fig. 3d is negative, which is due to the direct solar heating predominating in the summer hemisphere. The exceptions are: the troposphere, in which the temperature increases from both poles to the equator, the near-equatorial stratosphere, in which secondary circulation cells induced by the QBO contribute to the temperature regime (Dickinson, 1968 ; Choi et al., 2002 Fig. 3), and the MLT region, in which the positive gradient is explained by the predominance of the meridional atmosphere movement and adiabatic temperature adjustment caused by the vertical movements.

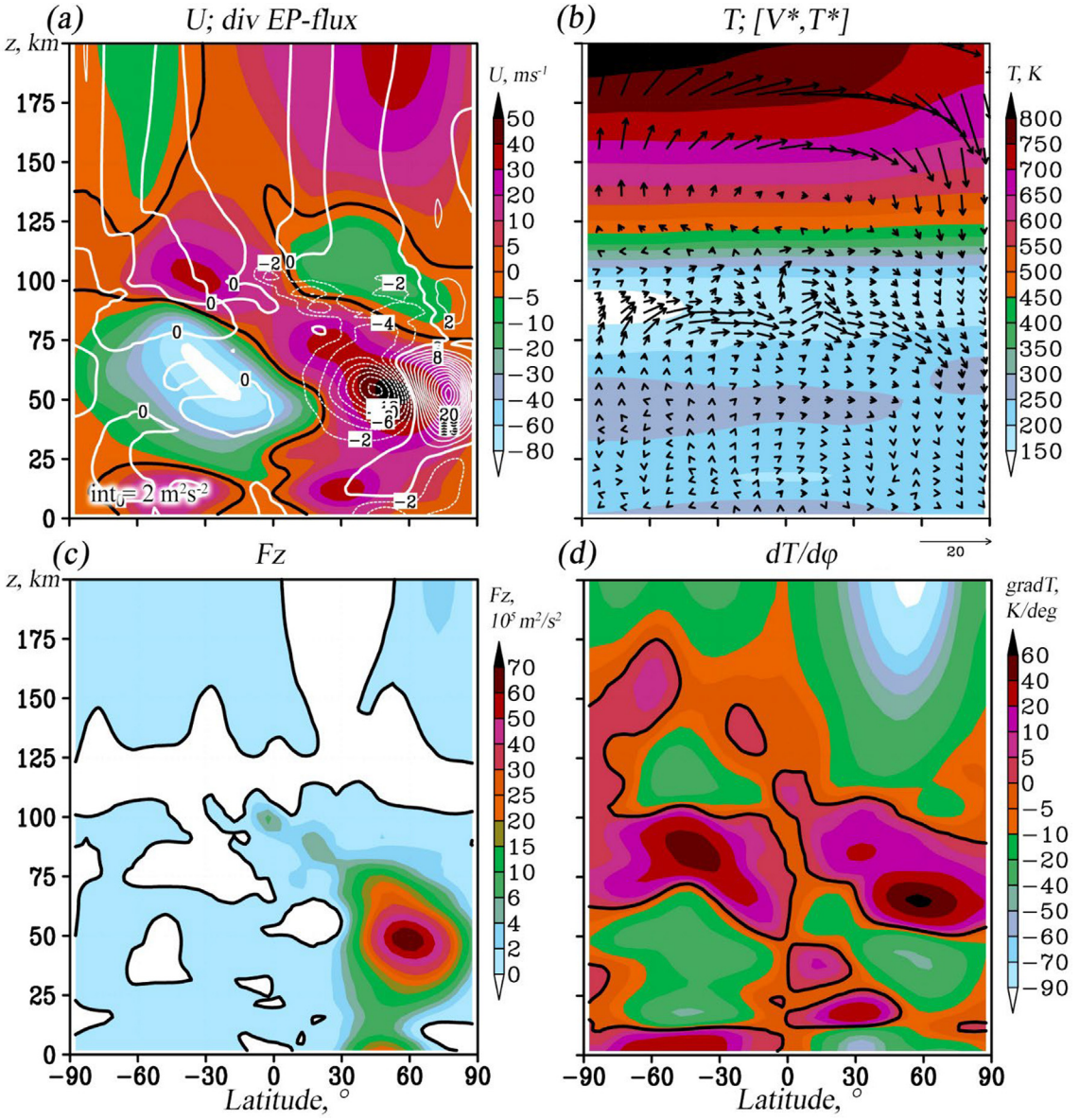

Fig. 3. WQBO latitude-altitude distributions of: (a) – zonal wind (shaded, m/s) and EP-flux divergence (contours, 10^2 m^2/s^2/day); (b) – temperature (shaded, K) and RMC components (arrows, m/s, vertical component multiplied by 200); (c) – vertical EP flux component (10^5 m^2/s^2); (d) – meridional temperature gradient (K/deg). All data is according to MUAM ensemble simulation for January.

Thus, we use the analysis of the EP flux divergence and changes in the meridional temperature gradients to interpret dynamic changes in the atmosphere, and the analysis of the RMC and vertical component of the EP flux to interpret temperature changes.

3.1. Thermal structure

Fig. 4 shows latitude-altitude distributions of differences in temperature (shaded) and RMC (arrows) between different QBO phases. In the equatorial region one can notice that the temperature anomalies gradually descend from phase to phase. In addition, at latitudes ± 20° – 50° in both hemispheres one can notice temperature anomalies of the opposite sign, which are formed due to the secondary meridional circulation cells considered above. At high northern latitudes, Fig. 4a shows the strongest increase in temperature of the stratosphere and cooling of the mesosphere (above 60 km) during the esQBO transition phase (from westerly to easterly QBO). During the next three phases (Fig. 4b-d), reverse processes in this area are predominating: cooling of the subpolar regions of the stratosphere and heating of the regions above and below this area. At the same time, these processes are much weaker than those in Fig. 4a. Thus, abrupt changes in the subpolar stratosphere during the esQBO are gradually compensated during the next 3 phases. If we compare the distributions of temperature increments in Fig. 4a-d with the distributions of the corresponding parameters according to the reanalysis data, shown with the contours in Fig. 1a-d, we observe

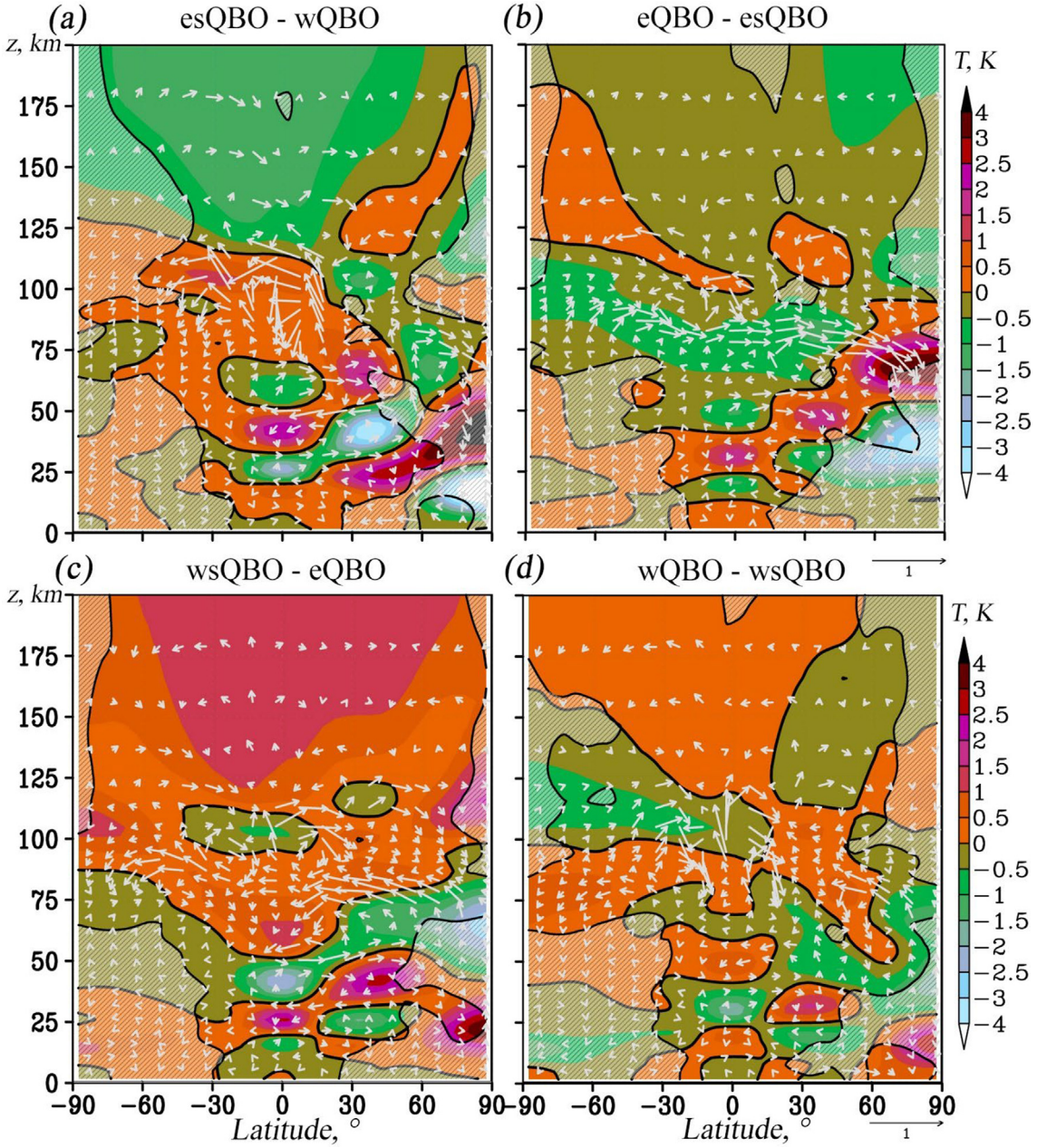

Fig. 4. Latitude-altitude distributions of differences between specified QBO phases in temperature (shaded, K) and RMC wind vectors (arrows, m/s) with vertical component multiplied by 200. Hatched areas show differences with statistical significance less than 95%.

similarities not only in the equatorial region (where nudging is used), but also at other latitudes. In particular, we observe anomalies associated with secondary circulation cells at latitudes of ± 20°−50°, the maximum change in temperature in the subpolar region are observed during the esQBO (Fig. 1a and 4a): warming above 25 km and cooling below this level. Some of the differences in tendencies, for example, in the circumpolar region between the Fig. 1b,c and 4b,c can be explained by two reasons: (i) we simulate the QBO effect in its pure form, all other parameters in the model remain identical, while in the real atmosphere (and reanalysis), in the selected years, a separate contribution could introduce other large-scale processes such as the El Niño Southern Oscillation, solar activity, etc.; (ii) in the circumpolar stratosphere, there may be discrepancies between the model and the reanalysis due to the presence/absence of sudden stratospheric warmings and their intensity. In general, we can conclude that the model satisfactorily reproduces the general circulation both in the tropics and in the extratropical region. And previous successful comparisons with semi-empirical models up to thermospheric heights (e.g., Koval et al. 2022a) allow us to analyze circulation up to 200 km.

The arrows in Fig. 4 show components of the RMC differences between respective QBO phases. As in the case of temperature changes, these increments in subpolar

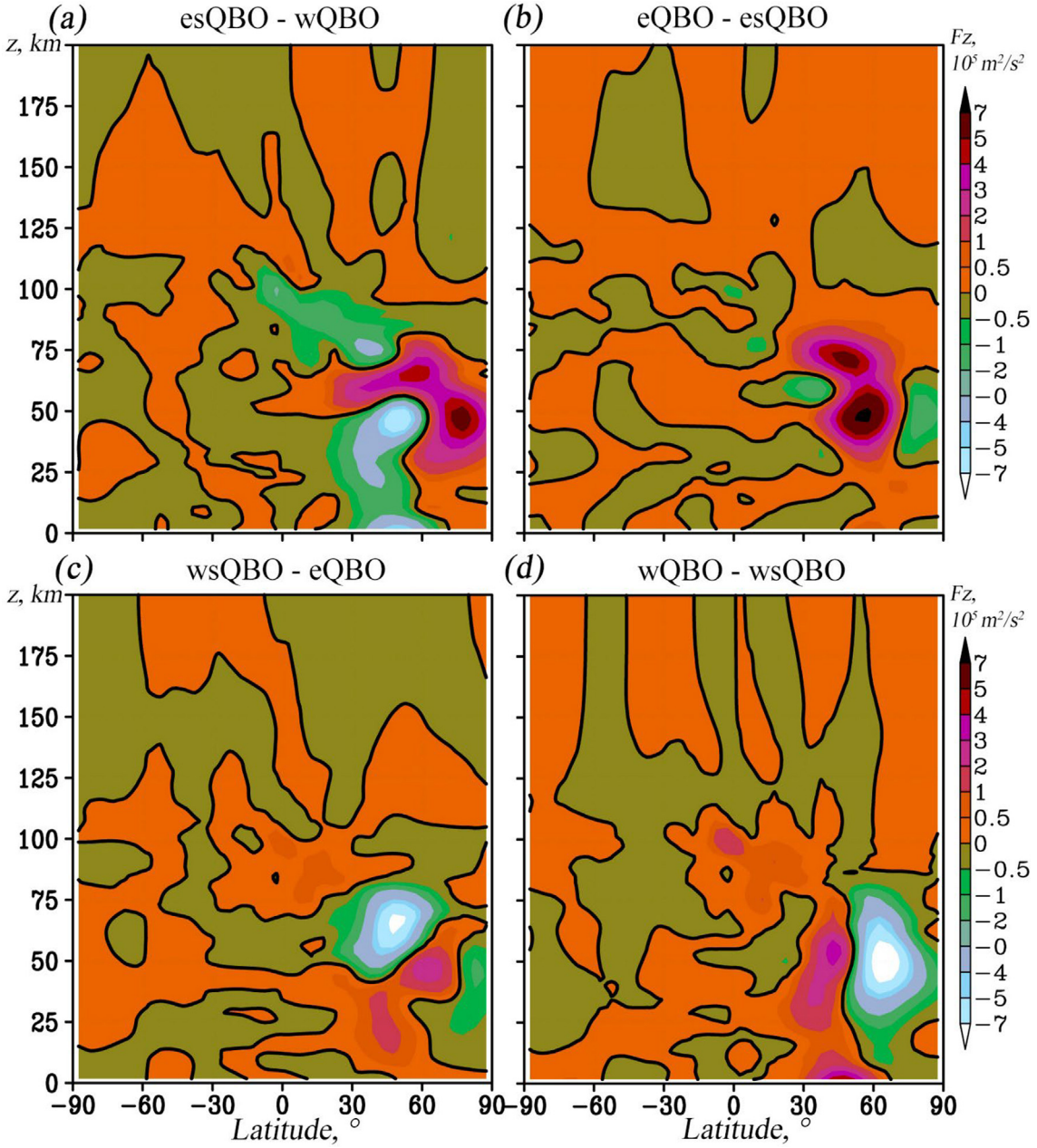

Fig. 5. Latitude-altitude distributions of vertical EP flux (10^5 m^2/s^2) differences between specified QBO phases.

stratosphere are maximum during the esQBO phase depicted in Fig. 4a. Increase and decrease in the vertical component of the RMC is accompanied, respectively, by adiabatic cooling and heating of atmospheric layers. The significant changes in the RMC are demonstrated also in the MLT area, in the altitude range of about 70–120 km in both hemispheres. In Fig. 4b and c, the change in the meridional component of RMC prevails in this area. During the remaining phases (Fig. 4a and d), the activation of vertical motions in the low-latitude region is noticeable. Together, these dynamic processes are associated with the changes in temperature profile of the lower thermosphere. In addition to the mentioned above adiabatic cooling/heating due to the vertical movement of air parcels peculiar to Fig. 4a and d, we observe cooling/heating of the lower thermosphere due to acceleration/deceleration of the meridional transfer of cold air masses from the Southern Hemisphere in Fig. 4b and c. In this context, we consider the relationship between the RMC and temperature as indirect evidence of the wave impact on atmospheric circulation, since meridional circulation is primarily generated by waves (e.g., Haynes et al., 1991).

Another mechanism which must be taken into account when analyzing temperature changes in the middle and upper atmosphere is the direct effect of PWs modulated by QBO. We consider this mechanism through the calculation of the vertical component of the EP flux, *Fz*. Latitude-altitude distributions of *Fz* increments (divided by density)

are shown in Fig. 5, while the *Fz* values themselves for all QBO phases are presented in Supplement, Fig. S2. The general structure of *Fz* is typical for the month of January: the maxima are observed in the winter middle atmosphere. In the thermosphere the EP flux weakens. If we compare Fig. 4a and 5a, it can be seen that significant increase in heating of the subpolar stratosphere during esQBO is directly associated with the wave action, since an increase in the upwardly directed EP flux causes a poleward wave heat flux (e.g., Andrews et al., 1987). The westerly QBO phase (Figs. 4d and 5d) is characterized by the same behavior but directed opposite: cooling of the high-latitude stratosphere and EP flux weakening. The fact that the wave activity in the extratropical region decreases (and the polar vortex intensifies) during wQBO is well-known (e.g., Baldwin et al., 2001; Anstey and Shepherd, 2014). During the remaining two phases, shown in Figs. 4-5b and c, *Fz* changes in the subpolar stratosphere decrease and hence direct PW effect weakens.

The statistical significance of the increments shown in Fig. 4 calculated using a paired Student's *t*-test applied to the above-mentioned 12-members ensembles of model simulations for each QBO phase. Statistically insignificant increments at the 95 % level are marked with diagonal hatching. It should be noted that in Fig. 4 hatching indicates statistically insignificant data on either temperature or RMC, i.e., outside the hatching, only significant increments are located.

During boreal winter, planetary waves effectively propagate upward from the troposphere to the Northern (winter) Hemisphere stratosphere through circulation structures when the zonal wind is eastward (e.g., Charney and Drazin, 1961). In the southern stratosphere, where PWs do not propagate during the boreal winter, significant changes in temperature and RMC are observed only at tropical latitudes, associated with secondary meridional circulation. In the MLT region, PW waveguides expand and PW propagate into the thermosphere in both hemispheres. This was shown repeatedly (e.g., Koval et al. 2018; 2019 and references therein). At the same time, it should be noted that the PWs under consideration are not capable of propagating directly into the thermosphere, since their waveguides are interrupted in the lower thermosphere. This can be demonstrated in Fig. 3c: above 100 km there is an area where the vertical EP flux tends to zero. Among the possible mechanisms of PW propagation into the thermosphere is the modulation of planetary waves by tides, considered in (Laštovicka, 2006) or by gravity waves (Hoffmann et al., 2012). Interacting with the mean flow, PWs have the maximum effect on the atmospheric circulation of the middle atmosphere of the winter hemisphere, where the amplitudes of most PWs modes are maximum. As the altitude increases, the influence of PW extends to both hemispheres, as demonstrated by Koval et al. (2019; 2022a). In the thermosphere, where other processes become relevant (e.g., chemical heating, ion-drag, molecular diffusion, solar activity), however, it is possible to observe statistically significant changes in the temperature and dynamic regimes, caused by the influence of PW. In particular, it can be seen that at altitudes above 100 km, cooling is generally observed during esQBO and eQBO (Fig. 4a and b), which is then replaced by an increase in temperature during wsQBO and partially during wQBO (Fig. 4c and d). At the same time, it is interesting that in the low-latitude thermosphere, cooling is accompanied by a weakening of vertical flows (in the Southern Hemisphere, ascending flows are weakening, and in the Northern Hemisphere, descending flows are weakening), while warming is accompanied by their intensification. It can be assumed that the increase in wave activity during esQBO and its weakening during wQBO leads, respectively, to the strengthening and weakening of the RMC in the thermosphere (above 130 km), shown in Fig. 4a and d.

3.2. Dynamic structure

Latitude-altitude structures of zonal-mean zonal wind increments due to a successive change in QBO phases are presented in Fig. 6. Respective values for all four QBO phases are shown in Supplement, Fig. S3. In order to analyze variations in the zonal flow, the following increments were calculated: EP flux divergence (represented by contours in Fig. 6) and meridional thermal gradient shown in Fig. 7. The statistical significance of the increments shown in Fig. 6 was calculated using a paired Student's *t*-test applied to the ensemble members of model simulations for each QBO phase. Statistically insignificant increments at the 95 % significance level are marked with diagonal hatching. The calculations showed that the statistical significance of the meridional gradient increments in Fig. 7 is greater than 95 % wherever the values exceed 0.3 K/deg, which is true for almost all distributions.

If we compare the simulated changes in the zonal wind in Fig. 6 with similar distributions constructed from the reanalysis data (Fig. 1, shading), we can conclude that the model satisfactorily reproduces the zonal circulation. Characteristic anomalies of the zonal wind in the equatorial stratosphere, which gradually, from phase to phase, shift down in Fig. 6a-d are observed. The maximum increment of the zonal wind is observed during the wsQBO in Fig. 6c, at an altitude of 25–35 km. In the subpolar stratosphere, the simulated tendencies also persist in the reanalysis: strengthening of the polar vortex during the esQBO (Fig. 6a), weakening – during the wsQBO and wQBO. The signal from 4 QBO phases in the extratropical region was studied in Solomon (2014) based on reanalysis and modeling. Despite the lack of statistical significance, the CAM5 model was shown to satisfactorily reproduce the QBO cycle. The trends in changes in, for example, the zonal wind and EP flux at stratosphere heights discussed in this work generally coincide with those calculated by us.

When discussing Figs. 4 and 5, we concluded that direct PW effect on the temperature regime of the subpolar

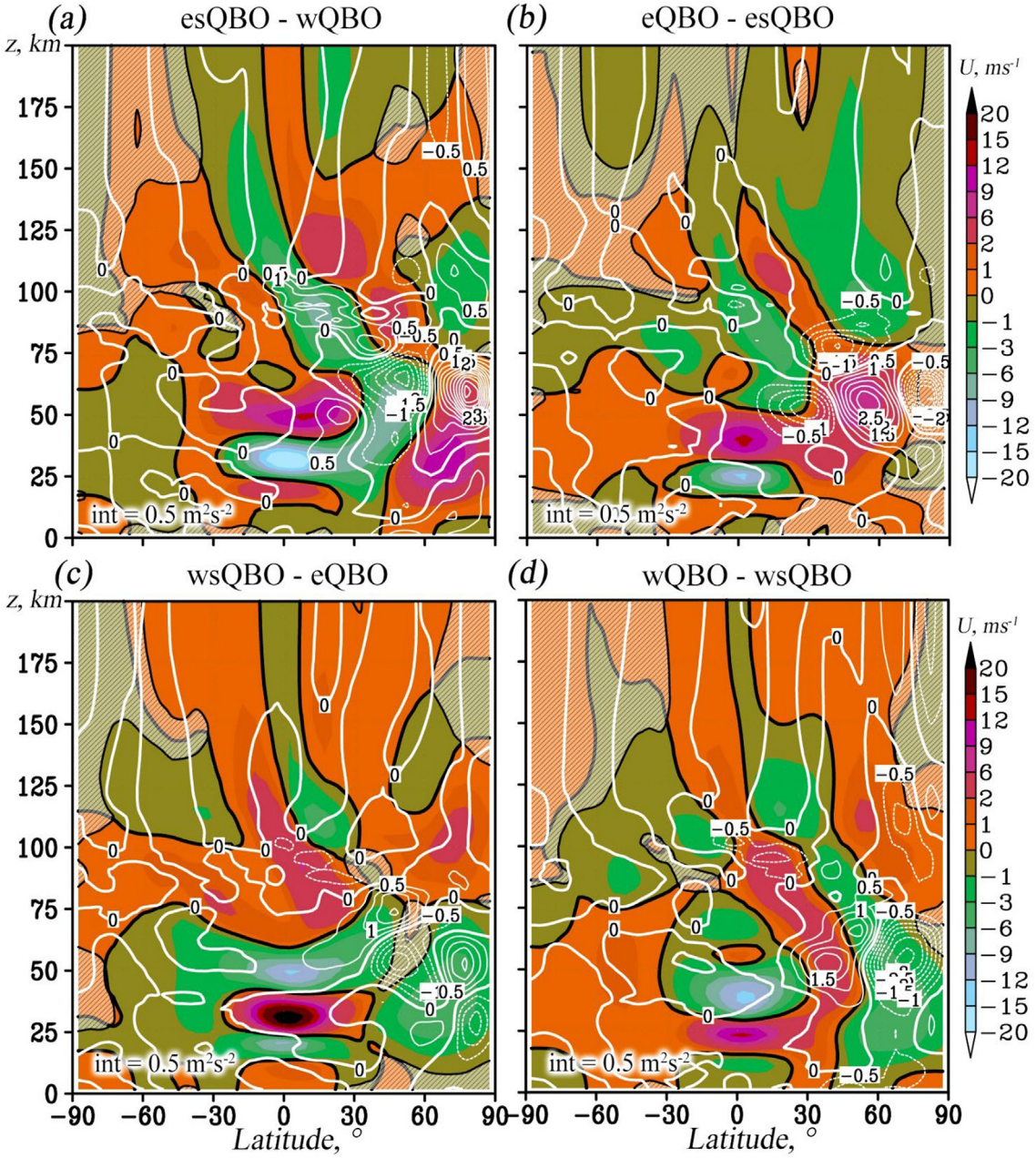

Fig. 6. Latitude-altitude distributions of differences between specified QBO phases in the zonal-mean zonal wind (shaded, m/s) and in the EP-flux divergence (contours, 10^2 m^2/s^2/day). Hatched areas show differences with statistical significance less than 95 %.

middle atmosphere is enhanced during the esQBO and wQBO, so we expect similar behavior when considering the zonal circulation. Indeed, in Fig. 6a and d, changes in the zonal wind in the extratropical middle atmosphere perfectly correspond to changes in the EP flux divergence. For example, in Fig. 6a, acceleration of the zonal wind in the northern stratosphere and deceleration at middle latitudes is related to the strengthening and weakening of the EP flux divergence in these regions. Similar but opposite correspondence is observed in the northern stratosphere during wQBO (Fig. 6d). It is interesting that in Fig. 6b and c, there is no such unambiguous correspondence between the zonal wind and the EP flux divergence, similar to situation observed in Figs. 4b,c and 5b,c. Again, PW activity decreases and direct PW impact weakens. However, if we compare the meridional circulation changes during these phases in Fig. 4b,c with the corresponding changes in the zonal wind, we see how the change in the meridional component of the RMC contributes to the change in the zonal wind: strengthening (weakening) of the meridional component in the upper stratosphere in Fig. 4b,c causes acceleration (deceleration) of the zonal wind through the Coriolis force. That is, the indirect effect of the PWs in this case dominates.

Hence, joint consideration of temperature increments and zonal circulation in Figs. 4 and 6 allows us to conclude

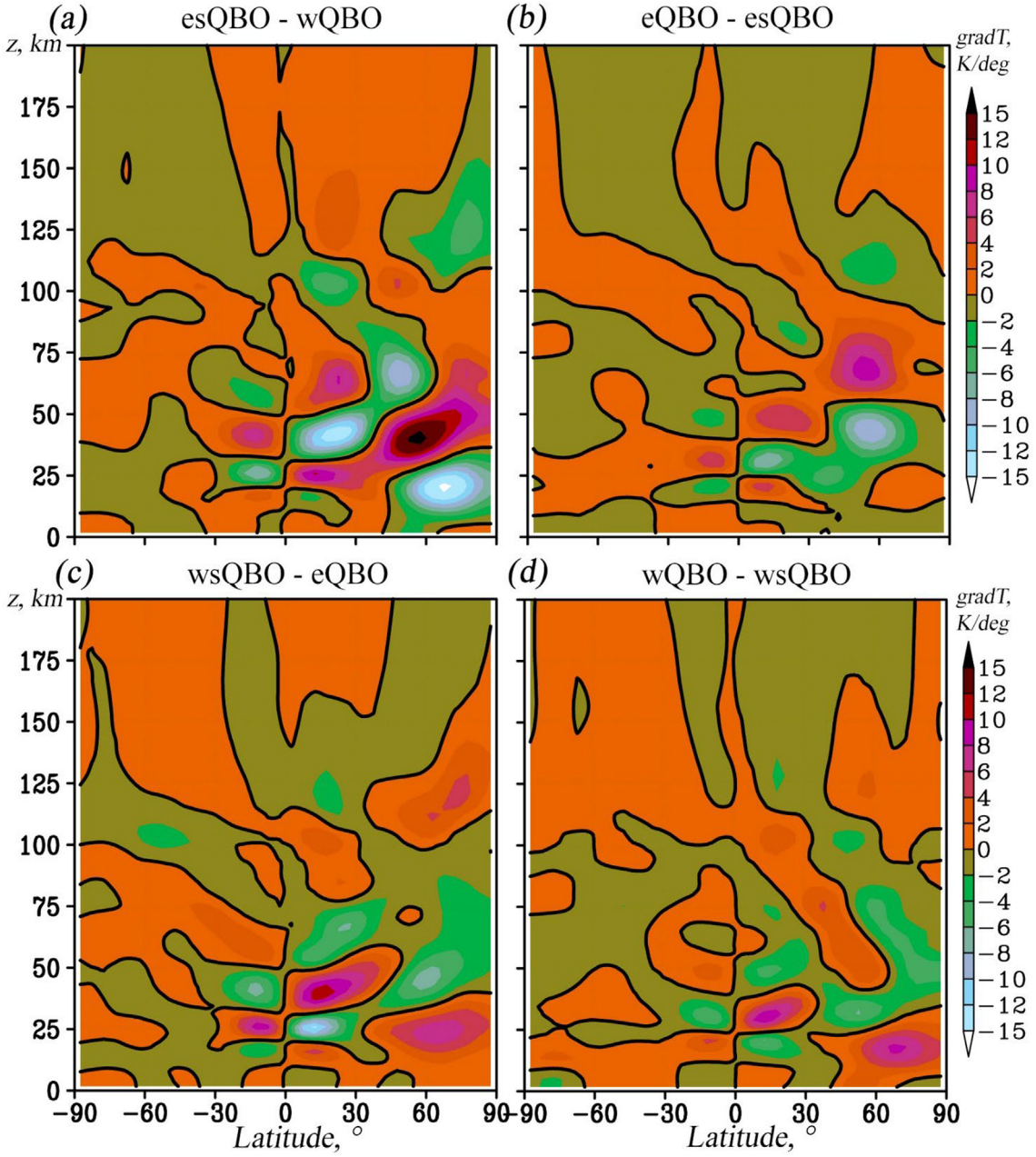

Fig. 7. Latitude-altitude distributions of differences in the meridional temperature gradients (K/deg) between specified QBO phases.

that the strongest and coldest polar vortex in the Arctic lower stratosphere is observed during the transitional esQBO phase, which is consistent with reanalysis data shown in Fig. 1. Above about 30 km, with an increase in altitude, the enhancement of the polar vortex continues during eQBO, which is caused by strengthening of the meridional RMC component. Simultaneously the wave activity in the upper northern stratosphere increases, accompanying by heating of the subpolar region of the stratosphere.

In the mid- and high-latitude regions of the southern stratosphere, we do not observe remarkable changes in the zonal wind in Fig. 6, as in the case of temperature and RMC in Fig. 4. Statistically significant increments of zonal wind and temperature can be seen in the MLT area and above. This confirms the fact that the QBO localized in the stratosphere can affect the circulation in the entire atmosphere. In particular, there is a weakening of the eastward and westward zonal wind in Fig. 6a in the tropics, in the altitude ranges of 75–100 km and 100–140 km, respectively, which coincide with the decrease in meridional transport in these regions, shown in Fig. 4a. As was discussed in Wang et al. (2017), the stratospheric QBO affects tidal amplitudes in the thermosphere, in particular, the strengthening of the amplitude of the diurnal tide in the total electron content and the weakening of the tide in

the temperature and wind fields at 97 km during the easterly phase were considered. A decrease in wave activity near this layer may contribute to the weakening of the RMC and, as a consequence, zonal flows. More or less clearly, such trends can also be traced at thermospheric heights during next, eQBO phase. Above approximately 130 km, the magnitude of changes in the zonal wind speed can reach 10 %, while with an increase in the wave activity in the Northern Hemisphere during the esQBO and eQBO (Fig. 6a), the zonal wind weakens, and during the ewQBO and wQBO, when the wave activity decrease, the zonal wind mainly intensifies. Although in general, as mentioned in the previous subsection, the purely dynamic effect of PWs and tides in the thermosphere can be much weaker than other processes that we did not take into account in this study, such as quasi-biennial variations in solar activity in the ionosphere.

Latitude-altitude distributions of differences in the meridional temperature gradients are shown in Fig. 7. According to the classic theory of thermal wind, the vertical gradient of zonal wind is proportional to the meridional temperature gradient. Poleward (positive in the Northern Hemisphere and negative in the Southern one) meridional temperature gradient should correspond to a westward vertical wind shear (e.g., Cai et al., 2022). So, increments of thermal meridional gradient in Fig. 7 correspond to the wind increments in Fig. 6 for all panels. In particular, weakening of the meridional temperature gradient in Fig. 7b below 50 km is associated with the increase in the zonal wind in this area. Above 50 km, with an increase in altitude, an increase in the gradient is related to the gradual weakening of the zonal wind. Similar but reversed properties can be seen in Figs. 6-7c. In the tropical region in Fig. 7, the increments of the meridional temperature gradient are arranged in a checkerboard pattern, reflecting cells of the meridional circulation symmetrical with respect to the equator, caused by the QBO.

It should be noted that the influence of other factors on the global circulation, for example, gravity waves (GWs) of orographic and non-orographic origin (e.g., Alexander and Holton, 1997; Yiğit and Medvedev, 2015), which are taken into account in the MUAM model using parameterizations and, thus, have a non-linear dependence on wind speed and direction and background temperature. Consideration of GW remained outside the scope of this study, because The TEM concept used, in accordance with the formulas used for calculating the EP flux and RMC, takes into account the waves resolved on the model grid: tides and PWs.

4. Discussion and conclusion

This study is the first attempt to consider in detail the peculiarities of large-scale atmospheric processes during the QBO transition phases. We investigate changes of the global circulation of the middle and upper atmosphere including the polar stratosphere and thermosphere at four different QBO phases. In order to carry out a detailed, statistically valid analysis, it is not enough to use observational information due to the limited time series of regular data, the presence of a relatively small number of recorded QBO cycles, and, most importantly, due to the variability of the QBO period and amplitude associated with the nonlinearity of the processes generating QBOs and interference with other processes (see, e.g., Huang et al. 2012). For this purpose, it is logical to use 2 possibilities: (i) the use of global circulation models capable of reproducing the QBO by running simulations for a long period up to hundreds of years (e.g., Andrews et al., 2019); (ii) perform idealized ensemble simulations using a mechanistic model of atmospheric circulation, fixing all other external factors that can impose their effects on the QBO (e.g., Pogoteltsev et al., 2007; Gavrilov et al., 2015). The second option is chosen in this paper using the MUAM numerical model. Simulations of the general circulation of the atmosphere from the surface to 200 km were carried out for conditions corresponding to four QBO phases observed in January at different years. To reproduce the QBO in the MUAM model, we used the procedure of nudging of the simulated wind and temperature fields in the equatorial stratosphere to the reanalysis data. In addition to the classical westerly and easterly QBO phases, transitional westerly-shear and easterly-shear QBO phases were considered. To study the thermal and dynamic regimes of the atmosphere, four 12-member ensembles of model simulations were obtained, corresponding to the considered QBO phases. In order to interpret the obtained changes in temperature and zonal wind, the residual meridional circulation, Eliassen-Palm flux, their divergence and meridional thermal gradients were calculated.

The considered interaction of planetary waves with the mean flow during different QBO phases can be conditionally divided into two processes: the direct impact of the PWs, which manifests itself in a change in the EP flux and its divergence, and indirect effect, through a change in the residual meridional circulation induced by waves. At the same time, it should be understood that all the processes under consideration are non-stationary and have feedback: PWs transmit a momentum flux to the mean flow, in turn, a change in circulation will change the PW waveguides, affecting PW spatio-temporal structure.

The first important result is that changes in temperature and zonal wind in the extratropical stratosphere occur unevenly. The esQBO transition phase (from westerly to easterly QBO) is characterized by the strongest temperature and zonal wind changes at middle and high northern latitudes (Note that our esQBO and eQBO phases roughly correspond to eQBO according to the widely used Singapore QBO index). This can be observed both from the simulation and from the reanalysis data. These changes are caused by both direct and indirect PW influence. Correspondence between the zonal wind changes in the extratropical middle atmosphere and changes in the EP flux divergence is clearly seen as well as correspondence

between changes in temperature and vertical EP flux component in the northern stratosphere. In addition to the direct effect of PWs, the amplification of circulation change during esQBO is caused by meridional circulation: anomalies associated with secondary circulation cells at latitudes of ± 20°−50° form increased northward meridional fluxes heating the subpolar stratosphere. Similar behavior was discussed earlier by Rao et al. (2020) based on SMIP5/6 models. Such RMC anomalies associated with QBO were shown also by Hitchman et al., (2021).

The abrupt changes in the subpolar stratosphere during esQBO are gradually compensated for the next 3 phases. Changes in temperature and zonal circulation, as a rule, have opposite signs, and the magnitude of the changes is smaller. Changes in circulation manifest either the effects of the meridional circulation (eQBO, wsQBO) or the direct PW effects (wQBO). In particular, for the eQBO and wsQBO there is no such unambiguous correspondence between global circulation and PW activity as for the esQBO and wQBO, but the relationship with the thermal regime of the atmosphere is more clearly traced.

Hence, the strongest and coldest polar vortex in the lower stratosphere is observed during the transitional esQBO phase, which is consistent with reanalysis data. It can be assumed that the observed attenuation of the polar vortex during the wsQBO, and especially the wQBO, when energy and momentum are transferred from the mean flow to the PW in the subpolar region (EP flux convergence), can provide better conditions for the onset of SSW events. However, further studies are required to confirm this hypothesis. On the contrary, a sharp intensification of the stratospheric polar vortex during the esQBO and its further intensification during the eQBO can lead to the isolation of the subpolar stratosphere and, consequently, contribute to the formation of ozone hole at the end of boreal winter during these phases.

In the southern stratosphere, where PWs do not propagate during the boreal winter, significant changes in temperature and RMC are observed only at tropical latitudes, associated with a secondary meridional circulation. Such mechanisms, involving adiabatic heating/cooling, were previously described by Choi et al. (2002); Ribera et al. (2004).

Significant changes in the temperature and zonal wind are demonstrated in the MLT area, in the altitude range of about 70–120 km in both hemispheres. During eQBO and wsQBO, the change in the meridional component of RMC causes acceleration/deceleration of the meridional transfer of cold air masses from the Southern Hemisphere resulting in cooling/heating of this layer. During the remaining phases, the activation of vertical motions in the low-latitude region is noticeable, leading to temperature changes through the adiabatic processes.

PWs effectively propagate upward from their tropospheric sources to the stratosphere of the winter hemisphere through circulation structures formed by westerly winds (e.g., Charney and Drazin, 1961). In the summer stratosphere in January, where zonal wind becomes easterly, PWs do not propagate. In the MLT region, PW waveguides expand southwards and PW propagate into the thermosphere in both hemispheres. This was shown both by the example of stationary PWs (Koval et al. 2019 and references therein) and westward propagating PWs (Koval et al., 2018). Interacting with the mean flow, PWs influence the middle atmospheric circulation of the winter hemisphere, where the amplitudes of most PW modes are maximum. In the thermosphere, the influence of PWs extends to both hemispheres, as was demonstrated by Koval et al. (2022a). This allowed statistically significant changes to be observed in the temperature and dynamic regimes, caused by the influence of PW and confirm the fact that the QBO localized in the stratosphere can affect the circulation in the entire atmosphere. In particular, one can see cooling in thermosphere during esQBO and eQBO, which is then replaced by an increase in temperature during wsQBO and partially during wQBO. In the low-latitude thermosphere, cooling is accompanied by a weakening of vertical flows, while warming is accompanied by their intensification. Changes in the zonal wind speed in the thermosphere due to the QBO phases changes can reach 10 %. Above approximately 150 km, an increase in wave activity in the Northern Hemisphere is accompanied by a weakening of the zonal wind during the esQBO and eQBO phases. In other phases, predominantly opposite tendencies are observed. As discussed in the study by Wang et al. (2018), at high solar activity, for example, the ionospheric quasi-biennial oscillation of solar activity becomes the dominant factor in the thermosphere, which in fact is able to camouflage the effect of the stratospheric QBO.

Availability of data and materials

According to the statement 1296 of the Civil Code of the Russian Federation, all rights on the MUAM code belong to the Russian State Hydrometeorological University (RSHU). To get access to the computer codes and for their usage a reader should get a permission from the RSHU Rector at the address 79, Voronezhskaya street, St. Petersburg, Russia, 192007, phone: 007 (812) 372-50-92. The authors will assist in getting such permission. The MERRA-2 reanalysis dataset can be obtained from https://disc.gsfc.nasa.gov/datasets/M2I6NVANA_5.12.4/summary. All plots in this study were made using Grid Analysis and Display System (GrADS) which is a free software developed by to the NASA Advanced Information Systems Research Program.

Declaration of competing interest

The authors declare that they have no known competing financial interests or personal relationships that could have appeared to influence the work reported in this paper.

Acknowledgements

The research was supported by the Saint Petersburg State University (research grant 116234986): numerical modeling of atmospheric circulation at various QBO phases, and by Russian Science Foundation (grant #24-17-00230): calculation of RMC and EP-fluxes, statistical analysis.

Appendix A. Supplementary material

Supplementary data to this article can be found online at https://doi.org/10.1016/j.asr.2024.07.037.

References

Alexander, M.J., Holton, J.R., 1997. A model study of zonal forcing in the equatorial stratosphere by convectively induced gravity waves. J. Atmos. Sci. 54, 408–419.

Alsepan, G., Lubis, S.W., Setiawan, S. 2016. Analysis of the Equatorial Lower Stratosphere Quasi-Biennial Oscillation (QBO) Using ECMWF-Interim Reanalysis Data Set. 2016 IOP Conf. Ser.: Earth Environ. Sci. 31, 012032, https://doi.org/10.1088/1755-1315/31/1/012032.

Andrews, D.G., Holton, J.R., Leovy, C.B., 1987. Middle atmosphere dynamics. Acad. Press, New York, p. 489.

Andrews, D.G., McIntyre, M.E., 1976. Planetary waves in horizontal and vertical shear: The generalized Eliassen-Palm relation and the mean zonal acceleration. J. Atmos. Sci. 33, 2031–2048. https://doi.org/10.1175/1520-0469(1976)033<2031:PWIHAV>2.0.CO;2.

Anstey, J.A., Shepherd, T.G., 2014. High-latitude influence of the quasi-biennial oscillation. Quart. J. Roy. Meteor. Soc. 140, 1–21. https://doi.org/10.1175/JAS-D-20-0248.1.

Baldwin, M.P., O'Sullivan, D., 1995. Stratospheric effects of ENSO-related tropospheric circulation anomalies. J. Clim. 4, 649–667.

Baldwin, M.P., Gray, L.J., Dunkerton, T.J., Hamilton, K., Haynes, P.H., Randel, W.J., Holton, J.R., Alexander, M.J., Hirota, I., Horinouchi, T., Jones, D.B.A., Kinnersley, J.S., Marquardt, C., Sato, K., Takahashi, M., 2001. The quasi-biennial oscillation. Rev. Geophys. 39 (2), 179–229.

Butchart, N., 2014. The Brewer-Dobson circulation. Rev. Geophys. 52, 157–184.

Cai, Q., Chen, W., Chen, S., Ma, T., Garfinkel, C.I., 2022. Influence of the Quasi-Biennial Oscillation on the spatial structure of the wintertime Arctic oscillation. J. Geophys. Res. Atmos. 127. https://doi.org/10.1029/2021JD035564 e2021JD035564.

Charney, J.G., Drazin, P.G., 1961. Propagation of planetary-scale disturbances from the lower into the upper atmosphere. J. Geophys. Res. 66, 83–109.

Choi, W., Lee, H., Grant, W.B., Park, J.H., Holton, J.R., Lee, K.M., Naujokat, B., 2002. On the secondary meridional circulation associated with the quasi-biennial oscillation. Tellus, Ser. B 54 (4), 395–406.

Dickinson, R.E., 1968. On the excitation and propagation of zonal winds in an atmosphere with Newtonian cooling. J. Atmos. Sci. 25, 269–279.

Drob, D.P., Emmert, J.T., Meriwether, J.W., Makela, J.J., Doornbos, E., Conde, M., Hernandez, G., Noto, G., Zawdie, K.A., McDonald, S.E., Huba, J.D., Klenzing, J.H., 2015. An update to the Horizontal Wind Model (HWM): The quiet time thermosphere. Earth Space Sci. 2, 301–319.

Ebel, A., Berger, U., Krueger, B.C., 1995. Numerical simulations with COMMA, a global model of the middle atmosphere // *SIMPO*. Newsletter 12, 22–32.

Echer, E., 2007. On the quasi-biennial oscillation (QBO) signal in the foF2 ionospheric parameter //. J. Atmos. Sol. Terr. Phys. 69, 621–627.

Emmert, J.T., Drob, D.P., Picone, J.M., Siskind, D.E., Jones Jr., M., Mlynczak, M.G., et al., 2020. NRLMSIS 2.0: A whole-atmosphere empirical model of temperature and neutral species densities. Earth Space Sci. 7 e2020EA001321.

Ermakova, T.S., Aniskina, O.G., Statnaya, I.A., Motsakov, M.A., Pogoreltsev, A.I., 2019. Simulation of the ENSO influence on the extra-tropical middle atmosphere. Earth Planets Space 71, 8. https://doi.org/10.1186/s40623-019-0987-9.

Fraedrich, K., Pawson, S., Wang, R., 1993. An EOF analysis of the vertical-time delay structure of the quasi-biennial oscillation. J. Atmos. Sci. 50 (20), 3357–3365.

Fröhlich, K., Pogoreltsev, A., Jacobi, Ch., 2003. Numerical simulation of tides, Rossby and Kelvin waves with the COMMA-LIM model. Adv. Space Res. 32, 863–868.

Gabriel, A., 2019. Long-term changes in the northern midwinter middle atmosphere in relation to the Quasi-Biennial Oscillation. J. Geophys. Res. Atmos. 124, 13914–13942. https://doi.org/10.1029/2019JD030679.

Garfinkel, C.I., Shaw, T.A., Hartmann, D.L., Waugh, D.W., 2012. Does the holton-tan mechanism explain how the quasi-biennial oscillation modulates the arctic polar vortex? J. Atmos. Sci. 69 (5), 1713–1733. https://doi.org/10.1175/JAS-D-11-0209.1.

Gavrilov, N.M., Koval, A.V., Pogoreltsev, A.I., Savenkova, E.N., 2015. Simulating influences of QBO phases and orographic gravity wave forcing on planetary waves in the middle atmosphere. Earth Planets Space 67, 86.

Gelaro, R., McCarty, W., Suárez, M.J., Todling, R., Molod, A., Takacs, L., et al., 2017. "The modern-era retrospective analysis for research and applications, version 2 (MERRA-2). J. Clim. 30 (14), 5419–5454.

Giorgetta, M., Jungclaus, J., Reick, C.H., Legutke, S., Bader, J., Böttinger, M., et al., 2013. Climate and carbon cycle changes from 1850 to 2100 in MPI-ESM simulations for the coupled model intercomparison project phase 5. J. Adv. Model. Earth Syst. 5, 572–597. https://doi.org/10.1002/jame.20038.

Hamilton, K., 1998. Effects of an imposed quasi-biennial oscillation in a comprehensive troposphere-stratosphere-mesosphere general circulation model. J. Atmos. Sci. 55, 2393–2418.

Haynes, P.H., McIntyre, M.E., Shepherd, T.G., Marks, C.J., Shine, K.P., 1991. On the "downward control" of extratropical diabatic circulations by eddy-induced mean zonal forces. J. Atmos. Sci. 48 (4), 651–678.

Hitchman, M.H., Yoden, S., Haynes, P.H., Kumar, V., Tegtmeier, S., 2021. An observational history of the direct influence of the stratospheric quasi-biennial oscillation on the tropical and subtropical upper troposphere and lower stratosphere. J. Meteorol. Soc. Jpn 99 (2), 239–267. https://doi.org/10.2151/jmsj.2021-012.

Hoffmann, P., Jacobi, Ch., Borries, C., 2012. A possible planetary wave coupling between the stratosphere and ionosphere by gravity wave modulation. J. Atmos. Solar-Terr. Phys. 75–76, 71–80 10.1016/j.jastp.2011.07.008.

Holton, J.R., Mass, C., 1976. Stratospheric vacillation cycles. J. Atmos. Sci. 33, 2218–12215.

Holton, J.R., Tan, H., 1980. The influence of the equatorial quasibiennial oscillation on the global circulation at 50 mb. J. Atmos. Sci. 37, 2200–2208.

Huang, B., Hu, Z.-Z., Kinter, J.L., Wu, Z., Kumar, A., 2012. Connection of stratospheric QBO with global atmospheric general circulation and tropical SST. Part I: Methodology and composite life cycle. Climate Dyn. 38, 1–23. https://doi.org/10.1007/s00382-011-1250-7.

Huesmann, A.S., Hitchman, M.H. 2001. The stratospheric quasi-biennial oscillation in the NCEP reanalyses: Climatological structures. J. Geophys. Res., 106, 11 859–11 874, https://doi.org/10.1029/2001JD900031.

Jacobi, Ch., Ermakova, T., Mewes, D., Pogoreltsev, A.I. 2017. El Niño influence on the mesosphere/lower thermosphere circulation at mid-latitudes as seen by a VHF meteor radar at Collm (51.3°N, 13°E). Adv. Radio Sci., 15, 199–206, 2017. https://doi.org/10.5194/ars-15-199-2017.

Koval, A. V., Gavrilov, N. M., Pogoreltsev, A. I., Shevchuk, N. O. (2018). Influence of solar activity on penetration of traveling planetary-scale waves from the troposphere into the thermosphere. Journal of Geophysical Research: Space Physics, 123. (8), 6888–6903, https://doi.org/10.1029/2018JA025680.

Koval, A.V., 2019. Statistically significant estimates of influence of solar activity on planetary waves in the middle atmosphere of the Northern Hemisphere as derived from MUAM model data. Solar-Terrestrial Physics. 5 (4), 53–59 10.12737/stp-54201907.

Koval, A.V., Didenko, K.A., Ermakova, T.S., Gavrilov, N.M., Kandieva, K.K. 2022b. Simulation of changes in the meridional circulation of the middle and upper atmosphere during transitional QBO phases // Proc. SPIE 12341, 28th International Symposium on Atmospheric and Ocean Optics: Atmospheric Physics, 1234170; https://doi.org/10.1117/12.2643046.

Koval, A.V., Gavrilov, N.M., Pogoreltsev, A.I., Shevchuk, N.O., 2019. Reactions of the middle atmosphere circulation and stationary planetary waves on the solar activity effects in the thermosphere. J. Geophys. Res. Space Phys. 124, 10645–10658. https://doi.org/10.1029/2019JA027392.

Koval, A.V., Chen, W., Didenko, K.A., Ermakova, T.S., Gavrilov, N.M., Pogoreltsev, A.I., Toptunova, O.N., Wei, K., Yarusova, A.N., Zarubin, A.S., 2021. Modelling the residual mean meridional circulation at different stages of sudden stratospheric warming events. Ann. Geophys. 39, 357–368. https://doi.org/10.5194/angeo-39-357-2021.

Koval, A.V., Gavrilov, N.M., Pogoreltsev, A.I., Kandieva, K.K., 2022a. Dynamical impacts of stratospheric QBO on the global circulation up to the lower thermosphere. J. Geophys. Res. Atmos. 127 e2021JD036095.

Laštovicka, J., 2006. Forcing of the ionosphere by waves from below. J. Atmos. Sol.-Terr. Phys. 68 (3), 479–497.

Pogoreltsev, A.I., 2007. Generation of normal atmospheric modes by stratospheric vacillations. Izvestiya Atmos. Ocean. Phys. 43 (4), 423–435. https://doi.org/10.1134/S0001433807040044.

Pogoreltsev, A.I., Vlasov, A.A., Fröhlich, K., Jacobi, Ch., 2007. Planetary waves in coupling the lower and upper atmosphere. J. Atmos. Solar-Terr. Phys. 69, 2083–2101. https://doi.org/10.1016/j.jastp.2007.05.014.

Pogoreltsev, A.I., Savenkova, E.N., Pertsev, N.N., 2014. Sudden stratospheric warmings: the role of normal atmospheric modes. Geomag. Aeron. 54 (2), 1–15.

Rao, J., Yu, Y.Y., Guo, D., Shi, C.H., Chen, D., Hu, D.Z., 2019. Evaluating the Brewer-Dobson circulation and its responses to ENSO, QBO, and the solar cycle in different reanalyses. Earth Planet. Phys. 3 (2), 166–181.

Ribera, P., Pena-Ortiz, C., Garcia-Herrera, R., Gallego, D., Gimeno, L., Hernandez, E., 2004. Detection of the secondary meridional circulation associated with the quasi-biennial oscillation. J. Geophys. Res. 109, D18112. https://doi.org/10.1029/2003JD004363.

Richter, J.H., Anstey, J.A., Butchart, N., Kawatani, Y., Meehl, G.A., Osprey, S., Simpson, I.R., 2020. Progress in simulating the quasi-biennial oscillation in CMIP models. Journal Geophysical Research: Atmospheres 125. https://doi.org/10.1029/2019JD032362 e2019JD032362.

Shepherd, T.G., 2007. Transport in the middle atmosphere. J. Meteor. Soc. Japan 85B, 165–191.

Solomon, A., Richter, J.H., Bacmeister, J.T., 2014. An objective analysis of the QBO in ERA-Interim and the Community Atmosphere Model, version 5. Geophys. Res. Lett. 41, 7791–7798. https://doi.org/10.1002/2014GL061801.

Suvorova, E.V., Pogoreltsev, A.I., 2011. Modeling of nonmigrating tides in the middle atmosphere. Geomagmetizm and Aeronomy. 51 (1), 105–115.

Trenberth, K.E., 1986. An assessment of the impact of transient eddies on the zonal mean flow during a blocking episode using localized Eliassen-Palm flux diagnostics. J. Atmos. Sci. 43, 2070–2087.

Wallace, J.M., Panetta, R.L., Estberg, J., 1993. Representation of the equatorial stratospheric quasi-biennial oscillation in EOF phase space. J. Atmos. Sci. 50, 1751–1762.

Wang, J.C., Tsai-Lin, R., Chang, L.C., Wuc, Q., Lin, C.C.H., Yue, J., 2018. Modeling study of the ionospheric responses to the quasi-biennial oscillations of the sun and stratosphere. J. Atmos. Sol. Terr. Phys. 171 (2018), 119–130.

White, I.P., Lu, H., Mitchell, N.J., Phillips, T., 2015. Dynamical response to the QBO in the northern winter stratosphere: Signatures in wave forcing and eddy fluxes of potential vorticity. J. Atmos. Sci. 72, 4487–4507. https://doi.org/10.1175/JAS-D-14-0358.1.

Yiğit, E., Medvedev, A.S., 2015. Internal wave coupling processes in Earth's atmosphere. Adv. Space Res. 55 (4), 983–1003. https://doi.org/10.1016/j.asr.2014.11.020.